

Numerical simulation of the hydrodynamical combustion to strange quark matter

Brian Niebergal,¹ Rachid Ouyed,¹ and Prashanth Jaikumar^{2,3}

¹*Department of Physics and Astronomy, University of Calgary, 2500 University Drive NW, Calgary, Alberta, T2N 1N4, Canada*

²*Department of Physics & Astronomy, California State University Long Beach, 1250 Bellflower Blvd., Long Beach, California 90840, USA*

³*Institute of Mathematical Sciences, C.I.T. Campus, Chennai, TN 600113, India*

(Received 4 September 2010; revised manuscript received 12 October 2010; published 17 December 2010)

We present results from a numerical solution to the burning of neutron matter inside a cold neutron star into stable u,d,s quark matter. Our method solves hydrodynamical flow equations in one dimension with neutrino emission from weak equilibrating reactions, and strange quark diffusion across the burning front. We also include entropy change from heat released in forming the stable quark phase. Our numerical results suggest burning front laminar speeds of 0.002–0.04 times the speed of light, much faster than previous estimates derived using only a reactive-diffusive description. Analytic solutions to hydrodynamical jump conditions with a temperature-dependent equation of state agree very well with our numerical findings for fluid velocities. The most important effect of neutrino cooling is that the conversion front stalls at lower density (below ≈ 2 times saturation density). In a two-dimensional setting, such rapid speeds and neutrino cooling may allow for a flame wrinkle instability to develop, possibly leading to detonation.

DOI: [10.1103/PhysRevC.82.062801](https://doi.org/10.1103/PhysRevC.82.062801)

PACS number(s): 97.60.Jd, 26.60.–c, 25.75.Nq

Introduction. On grounds of asymptotic freedom in quantum chromodynamics (QCD), hadronic matter subjected to high densities and/or temperatures will deconfine into a quark-gluon plasma. The low-density, high-temperature phase transition happened “in reverse” moments after the Big Bang, and was fleetingly seen in ultrarelativistic heavy-ion collision experiments (see [1] for a review). The high-density, low-temperature regime is relevant to compact stars. We assume the Witten hypothesis [2]: Bulk strange quark matter (henceforth SQM) is more stable than the nuclear world in which we live. The long lifetime of nuclei is reconciled as the improbability of $\approx A$ weak reactions to occur simultaneously in a nuclear volume containing A nucleons, but SQM can still exist in the form of strangelets or strange quark stars, and coexist with neutron stars [3]. Once SQM is nucleated inside a neutron star, how does it grow to form a strange quark star? In this paper, we numerically investigate the issue of combustion of pure neutron matter to u,d,s matter using hydrodynamics, taking into account binding energy release and neutrino emission across the burning front—going beyond previous treatments of the problem [4–9]. This problem is interesting for three main reasons: (i) In Type Ia supernovae, multidimensional studies of small scale dynamics of flame burning including turbulence provide support for a pathway to the distributed regime, which can be a platform for detonation of the white dwarf [10–12]. A delayed detonation model for Type Ia explosions has been discussed in the context of material unburnt by the initial deflagration [13]. Furthermore, deflagration-to-detonation (DDT) transition through turbulent flame burning in laboratory experiments on combustible gas mixtures was numerically studied [14]—all this naturally leads to an investigation of the existence of similar effects in SQM burning. (ii) Recent work on burning neutron matter to SQM [15] uses simple scaling arguments to show that the previously mentioned pathway to explosive detonation may occur for SQM burning in a neutron star, and (iii) explosive conversion of a neutron star to a strange quark star is astrophysically relevant, because it

was investigated as a model for gamma-ray bursts [16–20]. For SQM burning, far from turbulence-flame interactions, even the laminar flow was not analyzed in sufficient detail. Therefore, as a first step, in this work, we present an improved prescription of the burning front in the laminar flow approximation, and already find speeds as high as $\sim c/100$, where c denotes speed of light. This indicates that turbulent effects (such as those discussed in [15]) may well decide the fate of the conversion (deflagration or detonation). Consider the situation where a compact star’s central density has reached that of nuclear deconfinement, and SQM is seeded by one of many possible alternatives [21]. Recent studies investigated the consequences of such a transition occurring during the core-collapse phase of a supernova [22,23], or, if nucleation is delayed, in an older neutron star whose central density has increased because of spin-down [24]. The conversion scenario we consider is nonpremixed combustion [25] in a cold neutron star, where SQM (ash) initially grows from a seed by diffusion of strange quarks into neutron matter, viewed as a uniform (udd) mixture (fuel). The interface region attempts to equilibrate chemically by producing more strange quarks. Such a reactive-diffusive setup, assuming a constant-temperature zero-thickness interface, was first explored in [4]. We consider the case for a macroscopically thick interface, evolved with hydrodynamics, paying attention to the temperature gradient and neutrino emission. We find that a self-consistent numerical treatment increases the front velocity by 5–6 orders of magnitude over earlier analytic treatments [4,26]. This large difference is mostly from two assumptions made in previous analytic treatments: (i) considering the fluid and combustion speeds as equivalent, and (ii) linearization of the number density difference $n_d - n_s$ in the $d + u \leftrightarrow u + s$ reaction rate. Combustion inside a fluid involves flame propagation in most cases, requiring a hydrodynamical approach [9]. In addition to the usual conservation equations for the energy-momentum tensor, baryon number and electric charge, we also include a diffusion time scale for s quarks, neutrino emission,

and entropy evolution from change in internal energy from converting to SQM. In a typical combustion, local temperature increase and subsequent thermal diffusion controls the burning rate. However, in our situation, the thermal conductivity is small enough [27,28] that over the simulation time, the temperature gradient across the interface is unchanged. Surprisingly, this temperature variation becomes important through its effect on the pressure, not just reaction rates. We do not include dissipative terms in the hydrodynamical equations.

Microphysics—diffusion and reactions. We first introduce the inputs for the reactive-diffusive flow. Transport of d quarks (fuel) and s -quarks (ash) through the interface driven by concentration gradients results in colliding flows of different flavors. The diffusion coefficient relevant for burning into SQM is [27]

$$D \simeq 10^{-1} \left(\frac{\mu_f}{300 \text{ MeV}} \right)^{2/3} \left(\frac{T}{10 \text{ MeV}} \right)^{-5/3} \text{ cm}^2/s. \quad (1)$$

Equilibrium in SQM is established by beta decay and electron capture reactions,

$$d \rightarrow u + e^- + \bar{\nu}_e, \quad (2)$$

$$u + e^- \rightarrow d + \nu_e, \quad (3)$$

$$s \rightarrow u + e^- + \bar{\nu}_e, \quad (4)$$

$$u + e^- \rightarrow s + \nu_e, \quad (5)$$

$$d + u \leftrightarrow u + s. \quad (6)$$

We use rates given by [29], which also have equilibrium-seeking terms for the leptonic processes,

$$\Gamma_1 - \Gamma_2 = \frac{34}{5\pi} G_F^2 \cos^2 \theta_C \times p_F(d) p_F(u) T^4 (\mu_d - \mu_u - \mu_e)^2, \quad (7)$$

$$\Gamma_3 - \Gamma_4 = \frac{17}{40\pi} G_F^2 \sin^2 \theta_C \mu_s m_s^2 T^4 (\mu_s - \mu_u - \mu_e), \quad (8)$$

$$\Gamma_5 = \frac{16}{5\pi^5} G_F^2 \cos^2 \theta_C \sin^2 \theta_C \times p_F^2(u) p_F(d) p_F^2(s) \Delta\mu [\Delta\mu^2 + (4\pi T)^2], \quad (9)$$

where $\Delta\mu = (\mu_d - \mu_s)$, p_F is the quark's Fermi momentum, G_F Fermi's constant, and θ_C the Cabbibo angle. For process (6) to proceed in a given region, a minimum number of s quarks must be present. Although this number should depend on factors such as the strangelet mass and surface tension, here we simply make sure to avoid unphysical effects, such as superluminal diffusion speeds [30], by imposing a smooth cutoff on the s -quark Fermi momentum ($p_{F_s} = \sqrt{\mu_s^2 - m_s^2} \gtrsim 0.1 \text{ MeV}$) for reaction (6) to proceed (this is analogous to the activation temperature, in Arrhenius-type reactions, typically used in modeling heat-diffusion driven combustion).

Neutrino emission. Neutrinos are emitted copiously from the location of the interface, where the leptonic weak reaction rates from chemical equilibration are highest. At these temperatures (tens of MeV) and densities ($\rho \sim 10^{15} \text{ g/cc}$), neutrino mean free paths λ are on the order of 100 cm [31]. Accurate neutrino transport requires solving the Boltzmann equation,

which in our setup introduces additional stiffness in the flow equations. A simpler estimate capturing the essential physics in one dimension is to introduce an exponential cutoff on the neutrino emissivity as follows:

$$\varepsilon = (\varepsilon_{q\beta} + \varepsilon_{qs}) \times e^{-(x_1-x)/\lambda}, \quad (10)$$

where $\varepsilon_{q\beta}$ and ε_{qs} denote the nonequilibrium neutrino emission rate for reactions (2) and (4), respectively [29], x is the position of the emitting region, and x_1 is the position of the front of the burning interface. Effectively, for a given emitting region at x , if the distance to the interface $x_1 - x$ is more than the mean free path λ , then produced neutrinos are trapped; otherwise, they escape. Because $\lambda \sim 100 \text{ cm}$, neutrinos produced near or in the interface and directed outward essentially free stream. The matter ahead of the burning interface is cool, whereas SQM behind it is hot and produces many neutrinos. The small mean free path then implies that neutrino cooling does not significantly alter the temperature of equilibrated SQM on the time scale of the simulation, but has an important effect on the diffusion of strange quarks across the interface, and hence the speed of the burning front (Fig. 3).

Hydrodynamics. The one-dimensional (1D) hydrodynamical equations in our case are [30]

$$\frac{\partial U}{\partial t} = -\nabla F(U) + \mathcal{S}(U), \quad (11)$$

with variables,

$$U = \begin{pmatrix} n_s \\ n_s + n_d \\ n_s + n_d + n_u \\ hv \\ s \end{pmatrix}, \quad (12)$$

and corresponding advective-diffusive terms,

$$F(U) = \begin{pmatrix} vn_s + D\nabla n_s \\ v(n_s + n_d) \\ v(n_s + n_d + n_u) \\ hv^2 + P \\ vs \end{pmatrix}, \quad (13)$$

and source terms,

$$\mathcal{S}(U) = \begin{pmatrix} -\Gamma_3 + \Gamma_4 + \Gamma_5 \\ -\Gamma_1 + \Gamma_2 - \Gamma_3 + \Gamma_4 \\ 0 \\ 0 \\ -\frac{1}{T} \sum_i \mu_i \frac{dn_i}{dt} \end{pmatrix}. \quad (14)$$

Γ_{1-5} are reaction rates for processes in Eqs. (2)–(6) whereas index i in the entropy source term ranges over all the particles in the system $i = \{u, d, s, e^-, \nu\}$. Evolving entropy density s , rather than energy density, with a source term describing change in particle species [energy cost of “assembling” (u, d, s) matter], allows the binding energy of SQM to be self-consistently taken into account. The enthalpy h is convenient for fluids that are at relativistic densities. The fluid velocity

v is expressed in units of the speed of light. To solve this system numerically, we require a constitutive equation of state (EoS).

Equation of state. In this work we use the finite-temperature bag model $P = \frac{h}{4} - B$ for the EoS of SQM (neglecting the small electron pressure),

$$h = \frac{19}{9}\pi^2 T^4 + 2T^2 \sum_f \mu_f^2 + \frac{1}{\pi^2} \sum_f \mu_f^4, \quad (15)$$

$$s = \frac{\partial P}{\partial T}, n_f = \frac{\mu_f^3}{\pi^2} + \mu_f T^2. \quad (16)$$

The index f in the previous expressions indicates quark flavor (u, d, s). The same EoS is used for both the upstream (unburnt) and downstream (burnt) fluids, with the difference being that the upstream fluid is cold u, d matter, because at the point of burning, the neutrons are taken to be already dissolved into a u, d fluid (electron pressure is included). We will take up the case of a more complicated EoS, including mixed phases, in subsequent work.

Numerical simulations and results. The variables in the equations of hydrodynamical combustion [Eq. (12)] are solved for numerically. Time evolution is done using a fourth-order Runge-Kutta scheme, whereas spatially a third-order upwinded advection, flux-limited, finite-volume approach is used [32]. The diffusion and pressure gradient terms are second order, not upwinded, and treated separately from the advection terms (i.e., not flux limited). A large pressure wave is created from the initial state, even though it initially satisfies pressure equilibrium. This is typical for combustion problems, where the (unburnt) fluid in front of the interface is set in motion ([30], p. 487). However, this wave is transient and quickly flows past the burning region, increasing the speed of the interface without impacting its long-term evolution (for animations, visit <http://www.capca.ucalgary.ca>). An acceptable grid spacing is $\Delta x = 0.05$, resulting in a limited time step of $\Delta t/\Delta x < 0.3$ from the advection terms, and $\Delta t/(\Delta x)^2 < 1/D$ from the diffusion terms. For our small-scale simulations, diffusion rates are large enough close to the front that stiffness is not a serious issue. In stellar scale simulations, however, more elaborate numerical techniques would be required to resolve flame propagation [33]. Leaving more detailed description of numerical aspects to a subsequent article, we discuss here our main physical results.

- (i) Effects of hydrodynamics: In Fig. 1 the interface speed, with and without the effects of hydrodynamics, is plotted for various initial conversion densities. In the former case, typical speeds for the burning interface were found to be between $0.002c$ and $0.04c$ for initial baryon densities ranging from $1.7n_0$ to $5.3n_0$, where n_0 is nuclear saturation density. These burning speeds are much higher than previous estimates [4,26]. The reasons come from the T and μ_s variations across the finite-width interface. Just after contamination, at small values of μ_s , the reactions producing s quarks are dominated by the $\Delta\mu^3$ factor in Eq. (9). Further behind the interface, s -quark production becomes increasingly dependent on the temperature term. This increases the

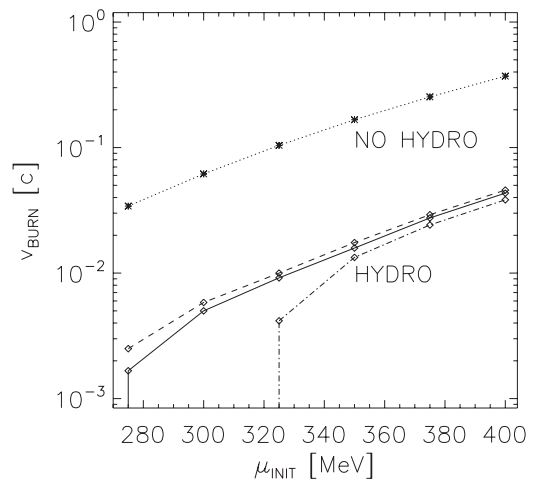


FIG. 1. Steady-state burning interface speeds v_{burn} for simulations with various initial densities (quark chemical potential) μ_{INIT} . The three hydrodynamic cases (HYDRO) are with no neutrino cooling (dashed line), neutrino cooling from Eq. (10) (solid line), and enhanced neutrino cooling (dash-dotted line). The dotted line indicates simulations without hydrodynamics (i.e., fluid velocities zero everywhere). v_{burn} increases with larger densities because more fuel is present, and decreases with larger cooling rates. As cooling becomes more effective, the hydrodynamic jump conditions [Eq. (A1)] are satisfied by increasingly opposing the advance of the interface, which consequently stalls at progressively higher densities.

reaction rate as expected [34], resulting in a faster speed of the burning interface. Including hydrodynamics in the reactive-diffusive simulations creates different fluid velocities on either side of the interface, which ends up effectively opposing the interface's progression (discussed later). Typical widths of the interface (see Fig. 2) were found to be ~ 1 cm when

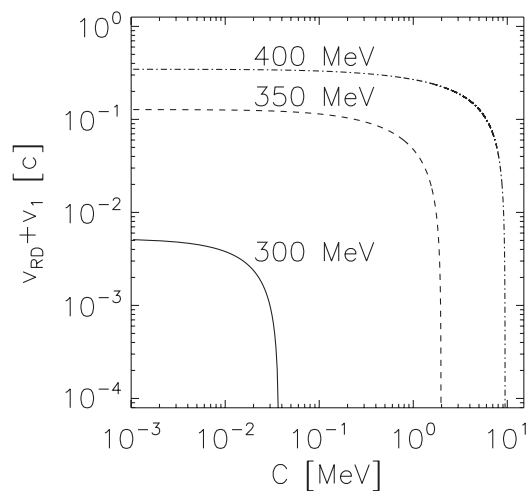


FIG. 2. A snapshot during the simulation of the temperature (T), reaction rate (R), and neutrino emissivity ϵ_ν throughout the burning interface. The temperature is shown with (solid line) and without (dashed line) neutrino cooling effects, where the difference between the two is the variable $C = T - T_{\text{cooled}}$ that serves as the measure of cooling.

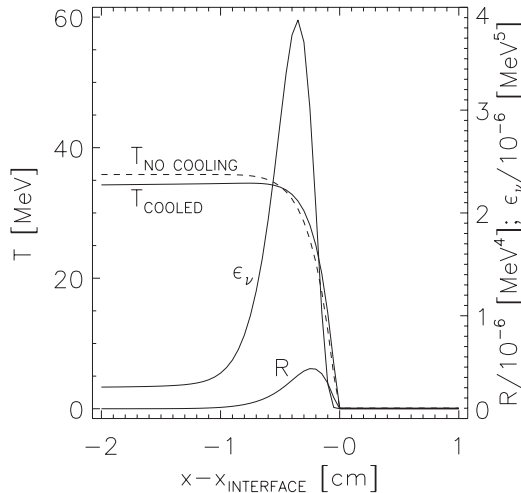


FIG. 3. Velocity of the burning interface, purely from the reaction-diffusion process (v_{RD} ; i.e., no hydrodynamics) plus the upstream fluid velocity (v_1), versus cooling. The upstream velocity is calculated analytically from the jump conditions (cf. Appendix), and neutrino cooling is represented by the difference between noncooled and cooled downstream temperatures $C = T - T_{\text{cooled}}$. Values shown are the initial densities. The interface halts after a critical amount of energy is removed by cooling.

hydrodynamics is included and ~ 10 cm for a purely reaction-diffusion system.

- (ii) Effects of ν cooling: Neutrino emission (deleptonization) causes a decrease in pressure for the burnt fluid. The resulting pressure gradient forces fluid velocities to become increasingly negative (in the reference frame comoving with the burning interface), causing advection to oppose the progression of the burning interface.¹ Because cooling rates may have uncertainties, we parametrize the efficacy of neutrino cooling by $C = T - T_{\text{cooled}}$, where T_{cooled} and T are the downstream (burnt) temperatures with and without cooling. As shown by the two temperature profiles in Fig. 2, even a modest drop in temperature can decrease the pressure enough to enter an advection dominated regime, where the upstream fluid velocity (v_1) advects the interface backward faster than it can progress from reactions and diffusion ($|v_1| > v_{RD}$). In such a case the interface halts, as seen in Fig. 3, as soon as $v_{RD} + v_1 < 0$. This is because as the interface stops diffusing into the fuel, the reactions are no longer proceeding. Because neutrino production drops as a consequence, energy is no longer being removed from the burning region and the system reaches a situation where diffusion and advection are in balance.

Discussion and conclusions. We have performed 1D numerical simulations of the burning of neutron matter to strange quark matter (SQM) with consistent treatment of

¹An analytic treatment using the jump conditions as described in the appendix confirms this effect.

reactions, diffusion, and hydrodynamics. We find typical speeds of the burning process to be between $0.002c$ and $0.04c$, which are noticeably higher than estimates found in previous works, for example, Refs. [6,27]. We have also shown how neutrino cooling can halt the burning interface by decreasing pressure support against advective forces. Hence, the importance of neutrinos cannot be overstated and must be addressed more thoroughly in future work. An equally important focus for future work is a two-dimensional treatment. Although cooling can only halt the interface in one dimension, in two or more dimensions we propose that a new type of instability would develop, caused by regions along the burning interface halting from cooling, at which point unburnt material starts to flow backward onto the interface, whereas regions not halted by cooling will have unburnt material flowing away from the interface. The result is a wrinkled interface that increases the diffusion rate, causing an overall increase in the burning interface's speed (v_{burn}). However, the wrinkling is also subject to stabilization by diffusion—concave regions of the interface are accelerated whereas convex regions are decelerated. The interplay between stabilization and the wrinkling instability can result in three scenarios: Either (i) stabilization is too strong causing v_{burn} to remain small and the entire interface halts, or (ii) stabilization is moderate and the interface progresses outward as a combustion, or (iii) stabilization is weak and v_{burn} increases without bound, presumably resulting in a detonation. Validating these options would require high-resolution multidimensional simulations, which we leave for future work, but related astrophysical applications worth mentioning here are: (i) inner engines of gamma-ray bursts driven by conversion of neutron stars to quark stars [16–20]; (ii) photometry and spectrometry of superluminous supernovae [35]; and (iii) r -process nucleosynthesis from decompressing neutron star crusts [36] ejected by a detonation.

Acknowledgments. This research is supported by grants from the Natural Science and Engineering Research Council of Canada (NSERC) and Alberta Innovates (iCore).

Appendix: Verification of numerical solutions. The reactive part of the code agrees well with analytically estimated time scales for achieving weak equilibrium [4,29,34]. For hydrodynamics, we solved the hydrodynamic jump conditions analytically in the frame of the burning interface. From Eq. (13),

$$(\mu_{u,1}^3 + \mu_{d,1}^3)v_1 = (\mu_{u,2}^3 + \mu_{d,2}^3 + \mu_{s,2}^3)v_2 \quad (\text{A1})$$

$$h_1 v_1^2 + P_1 = h_2 v_2^2 + P_2. \quad (\text{A2})$$

The subscripts 1 and 2 indicate upstream (unburnt) and downstream (burnt) fluids, respectively. Pressure is given in terms of enthalpy (Eq. (15)). The previous expressions are solved analytically, and upstream and downstream velocities agree to better than 2% with those found numerically. We do not include the jump condition from the entropy equation, because the reaction term introduces a nonlinear component, so the temperature increase from release of binding energy is not found analytically. Instead, we used computed values from simulations without hydrodynamics.

- [1] P. Braun-Munzinger and J. Stachel, *Nature (London)* **448**, 302 (2007).
- [2] E. Witten, *Phys. Rev. D* **30**, 272 (1984).
- [3] A. Bauswein, H. Janka, R. Oechslin, G. Pagliara, I. Sagert, J. Schaffner-Bielich, M. M. Hohle, and R. Neuhaeuser, *Phys. Rev. Lett.* **103**, 011101 (2009).
- [4] A. V. Olinto, *Phys. Lett. B* **192**, 71 (1987).
- [5] J. E. Horvath and O. G. Benvenuto, *Phys. Lett. B* **213**, 516 (1988).
- [6] M. L. Olesen and J. Madsen, *Nucl. Phys. B, Proc. Suppl.* **24**, 170 (1991).
- [7] H. T. Cho, K. Ng, and A. D. Speliotopoulos, *Phys. Lett. B* **326**, 111 (1994).
- [8] G. Lugones, O. G. Benvenuto, and H. Vucetich, *Phys. Rev. D* **50**, 6100 (1994).
- [9] A. Drago, A. Lavagno, and I. Parenti, *Astrophys. J.* **659**, 1519 (2007).
- [10] A. J. Aspden, J. B. Bell, M. S. Day, S. E. Woosley, and M. Zingale, *Astrophys. J.* **689**, 1173 (2008).
- [11] S. E. Woosley, A. R. Kerstein, V. Sankaran, A. J. Aspden, and F. K. Röpke, *Astrophys. J.* **704**, 255 (2009).
- [12] L. Pan, J. C. Wheeler, and J. Scalzo, *Astrophys. J.* **681**, 470 (2008).
- [13] V. N. Gamezo, A. M. Khokhlov, and E. S. Oran, *Astrophys. J.* **623**, 337 (2005).
- [14] A. M. Khokhlov, E. S. Oran, and G. O. Thomas, *Combust. Flame* **117**, 323 (1999).
- [15] J. E. Horvath, [arXiv:1005.4302v1](https://arxiv.org/abs/1005.4302v1).
- [16] G. Lugones, C. R. Ghezzi, E. M. de Gouveia Dal Pino, and J. E. Horvath, *Astrophys. J.* **581**, L101 (2002).
- [17] R. Ouyed and F. Sannino, *Astron. Astrophys.* **387**, 725 (2002).
- [18] Z. Berezhiani, I. Bombaci, A. Drago, F. Frontera, and A. Lavagno, *Nucl. Phys. B: Proc. Suppl.* **113**, 268 (2002).
- [19] P. Haensel and J. L. Zdunik, *Nuovo Cimento B* **121**, 1349 (2006).
- [20] A. Drago, G. Pagliara, and J. Schaffner-Bielich, *J. Phys. G* **35**, 014052 (2008).
- [21] C. Alcock, E. Farhi, and A. Olinto, *Astrophys. J.* **310**, 261 (1986).
- [22] I. Sagert, T. Fischer, M. Hempel, G. Pagliara, J. Schaffner-Bielich, A. Mezzacappa, F. Thielemann, and M. Liebendörfer, *Phys. Rev. Lett.* **102**, 081101 (2009).
- [23] B. Dasgupta, T. Fischer, S. Horiuchi, M. Liebendörfer, A. Mirizzi, I. Sagert, and J. Schaffner-Bielich, *Phys. Rev. D* **81**, 103005 (2010).
- [24] J. E. Staff, R. Ouyed, and P. Jaikumar, *Astrophys. J.* **645**, L145 (2006).
- [25] N. Peters, *Turbulent Combustion* (Cambridge University Press, Cambridge, 2000).
- [26] H. Heiselberg, G. Baym, and C. J. Pethick, *Nucl. Phys. B: Proc. Suppl.* **24**, 144 (1991).
- [27] H. Heiselberg and C. J. Pethick, *Phys. Rev. D* **48**, 2916 (1993).
- [28] V. V. Usov, *Astrophys. J.* **559**, L135 (2001).
- [29] J. D. Anand, A. Goyal, V. K. Gupta, and S. Singh, *Astrophys. J.* **481**, 954 (1997).
- [30] L. D. Landau and E. M. Lifshitz, *Course of Theoretical Physics* (Pergamon Press, Oxford, 1959).
- [31] N. Iwamoto, *Ann. Phys.* **141**, 1 (1982).
- [32] R. J. Leveque, in *Saas-Fee Advanced Course 27: Computational Methods for Astrophysical Fluid Flow*, edited by O. Steiner and A. Gautschy (Springer, New York, 1998), p. 1.
- [33] M. Zingale, A. S. Almgren, J. B. Bell, M. S. Day, C. A. Rendleman, and S. E. Woosley, *J. Phys. Conf. Ser.* **46**, 385 (2006).
- [34] J. Madsen, *Phys. Rev. D* **47**, 325 (1993).
- [35] D. Leahy and R. Ouyed, *MNRAS* **387**, 1193 (2008).
- [36] P. Jaikumar, B. S. Meyer, K. Otsuki, and R. Ouyed, *Astron. Astrophys.* **471**, 227 (2007).